

## Two Case Studies of Wintertime Cloud Systems over the Colorado Rockies

ROBERT R. LEE<sup>1</sup>

*Department of Atmospheric Science, Colorado State University, Fort Collins, CO 80523*

(Manuscript received 1 August 1983, in final form 14 November 1983)

### ABSTRACT

The economical importance of the winter snowpack to the Colorado Rocky Mountain region (e.g., weather modification potential, ski industry, avalanche prediction, snow removal, etc.) calls for an understanding of how the mountain environment and synoptic weather systems interact to produce precipitating orographic cloud systems. This may be achieved by recognizing that each cloud system can be broken down into individual cloud components. In each of the case studies, a synoptic cloud component, an orographic cloud component, and a convective cloud component were identified through the analysis of rawinsonde data, vertically pointing radar data, and visual observations.

This study shows that wintertime cloud systems over mountainous terrain can be thought of as being composed of cloud components that form when vertical velocity components act on different size and time scales (synoptic, orographic, convective). The following atmospheric phenomena are shown to be important factors which contribute to wintertime orographic systems: 1) a fourth cloud forming component, 2) upwind blocking, and 3) airflow saturation. At times, a fourth cloud component, generated by the mesoscale structure of the synoptic disturbance (e.g., traveling gravity waves, moving convective bands, or organized convective lines, etc.) invigorates the entire cloud system. The orographic lift and the orographic cloud component are strongly affected by any region of stagnant air that extends upwind of the mountain ridge, i.e., upwind blocking. The orographic cloud component is also very sensitive to 1) the manner in which the upwind air is lifted and 2) the upwind profiles of temperature and moisture.

### 1. Introduction

The formation of many orographic cloud systems can be attributed to the passage of synoptic scale migratory waves. These atmospheric disturbances provide the moisture and circulation, when sufficiently forced by the mountains, to form this type of cloud system. This is especially true of continental orographic cloud systems which play a significant role in establishing the winter snowpack in the Colorado Rocky Mountain region.

Precipitation in mountainous terrain can be thought of as being made up of three components: 1) the synoptic precipitation, 2) the orographic precipitation, and 3) the convective precipitation. These three components are directly related to the vertical motion fields associated, respectively, with migratory waves, terrain lifting and the local release of convective instability (Elliott, 1966; Rhea, 1978). Visual observations by Marwitz (1974) and precipitation network analysis by Elliott and Schaffer (1962) and Elliott and Hovind (1964) point to the existence of these three precipitation components and their corresponding vertical velocity fields.

This paper proposes to identify the principle mechanisms by which mountains and synoptic weather systems interact to produce characteristic cold orographic cloud systems. This goal is achieved by analyzing synoptic, orographic, and convective cloud components from two wintertime cloud systems that formed over the Colorado Rockies.

### 2. Data

In order to investigate the interaction of the orography with the synoptic scale wave, case studies were selected to describe different cloud systems and their accompanying atmospheric disturbances. Data collected during the Colorado State University Orographic Seeding Experiments (COSE-I—January, February and March 1979 and COSE-II—November and December 1979), conducted throughout the Yampa Valley and over the Park Range of northwestern Colorado, shape the basis of these case studies (see Fig. 1). Rawinsonde data,  $K_u$  band ( $\lambda = 1.8$  cm) and  $K_a$  band ( $\lambda = 0.8$  cm) radar data and observations of precipitation across the barrier were used to describe each case study cloud system. Rawinsondes were launched from the Craig airport (surface elevation, 1886 m) and the radars were stationed southeast of Steamboat Springs at the upwind base of the mountain barrier (see Fig. 2). Fig. 3 illustrates the topographic cross section from Craig to the

<sup>1</sup> Present affiliation: Air Force Geophysics Laboratory: AFGL/LYC, Hanscom AFB, MA 01731.

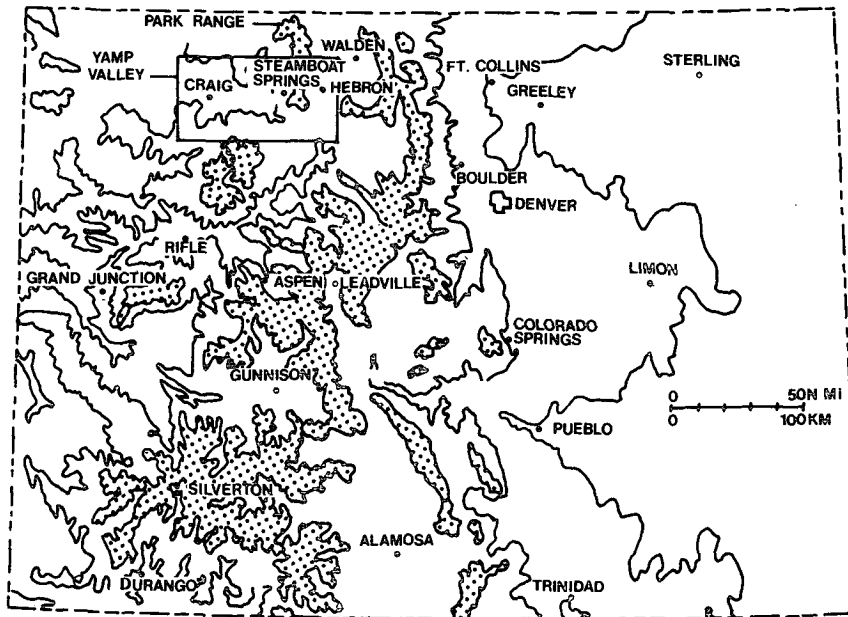


FIG. 1. The state of Colorado and the COSE study area. Stippling indicates elevations over 10 000 feet.

barrier crest and the positions at which the rawinsonde data, radar data, visual observations and the precipitation data were collected.

3. Analysis methods

The following definitions will be used in this paper:

- Synoptic cloud component—The portion of the cloud system which formed upwind of the Park Range barrier due to vertical air motions induced by differential vorticity advection or frontal lifting.

- Orographic cloud component—The portion of the cloud system which formed due to vertical velocities induced by orographic lifting of the air over the Park Range barrier.

- Convective cloud component—The portion of the cloud system in which convective motions were expected to occur by the release of potential convective instability; i.e., if a potentially unstable layer,  $d\theta_e/dZ < 0$ , is brought to water saturation then that layer will become unstable (Saucier, 1955).

- Synoptic scale vertical velocity components—

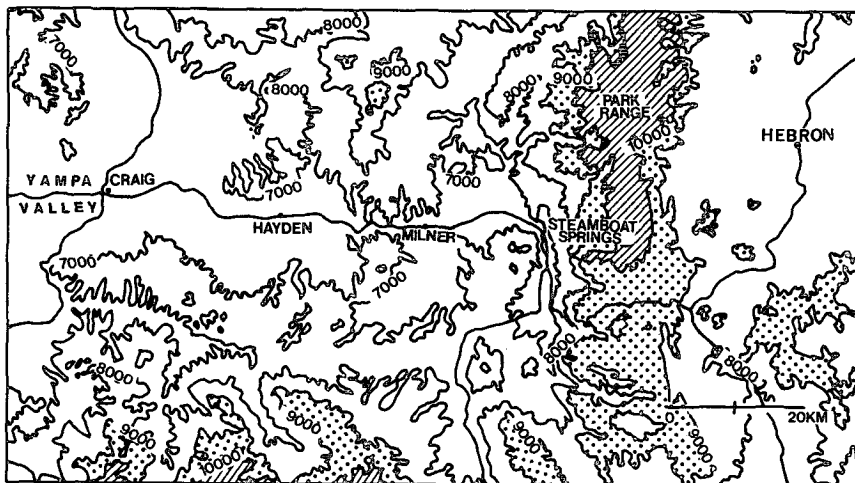


FIG. 2. The COSE study area: Yampa Valley and Park Range. The stipples indicate elevations over 9000 feet and the cross hatching indicates elevations over 10 000 feet.

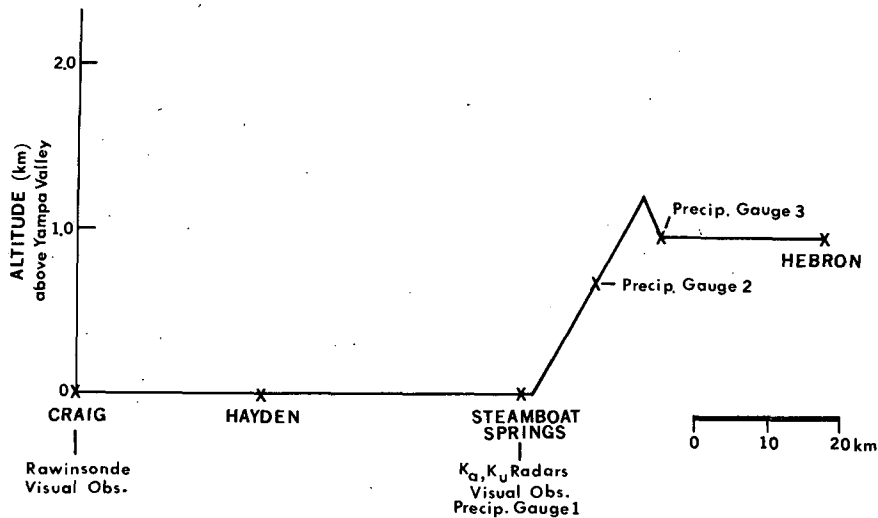


FIG. 3. Cross section of the X-Z topography for the COSE study area.

about  $0.1 \text{ m s}^{-1}$ , are determined by differential vorticity advection and air mass lifting by frontal systems. An existing orographic cloud may be enhanced by the synoptic vertical velocity field ahead of the upper level atmospheric disturbance or suppressed by subsidence behind the trough.

- Orographic vertical velocity components—about  $0.3 \text{ m s}^{-1}$ , (stable air forced vertically by the topography) are the dominant components in that they provide a more persistent vertical velocity field in time. As air mass stability changes, the dynamics of the orographic airflow are changed and the convective component establishes itself.

- The convective vertical velocity components—about  $1 \text{ m s}^{-1}$ , are important because they can physically alter the spacial and microphysical structure of an otherwise stable cloud system. Convection superimposed on a smooth orographic airflow will also have a large effect on the flow pattern.

These last three components can be identified as separate units but they combine and interact with each other. The degree of interaction ultimately determines the characteristics of each individual orographic cloud system.

There are many ways to define a “cloud” from rawinsonde data. Water saturation, ice saturation, a threshold dew-point depression or an arbitrarily defined relative humidity value are a few of the criteria used. In order to illustrate this difficulty, cloud tops from the 0000 and 0300 GMT soundings from Case Study 1 were determined using different criteria and are presented in Table 1. Because cloud areas cannot accurately be determined directly from rawinsonde data alone, an attempt will be made to define the cloud region from a best case–worst case approach.

In this study, “cloud boundaries”, bases and tops,

were theoretically defined to exist between ice saturation and water saturation. For example, consider a wintertime sounding (surface temperature =  $-10^\circ\text{C}$ ) in which the relative humidity is 20% at the surface, steadily increases to 100% at 70 kPa, remains at 100% to 60 kPa, and then steadily decreases to 10% at 20 kPa. To determine an estimate of actual cloud base, begin at the surface and search upwards through the sounding until ice saturation is reached. This is the ice saturated cloud base. Continue searching upwards through the layers supersaturated with respect to ice until water saturation is reached (70 kPa). This is water saturated cloud base. The actual cloud base should lie somewhere between the ice saturated cloud base and the water saturated cloud base. The estimate of actual cloud top is determined in the same manner. Continue searching upwards to find water saturated cloud top (60 kPa) and then ice saturated cloud top. Again, actual cloud tops should be somewhere between the two saturation levels.

The points of ice saturation and water saturation will only give lower and upper estimates of the actual cloud boundaries from the rawinsonde data. When the ice saturation and water saturation points are close together, a good estimate of actual cloud boundaries

TABLE 1. Various cloud top pressures as determined from different cloud top criteria (units in kPa).

	Relative humidity		Dew-point depression			Ice saturation
	80%	85%	2°C	3°C	4°C	
0000 GMT	35.0	36.3	35.5	37.0	24.0	25.0
0003 GMT	38.0	40.0	40.0	35.0	25.0	25.0

results. However, when the two saturation points are far apart, it is difficult to determine where the actual cloud boundaries exist. This latter cloud condition occurs for cloud tops from 1800 GMT 22 February to 1200 GMT 23 February and again from 1800 GMT 23 February to 0600 GMT 24 February in Figs. 7a and 7b (Section 4). In addition to rawinsonde analysis, visual observations were also used to qualitatively describe cloud structure and verify when the various cloud components were present.

The synoptic cloud components were identified as those layers within the upwind, unlifted soundings that were saturated with respect to ice and water. The majority of the unlifted soundings consisted of ice saturated layers only.

The soundings had to be lifted in a manner that simulated the airflow over the mountain barrier before the orographic cloud component could be defined. The orographic lift is contingent upon the transbarrier wind component, the temperature structure of the lower layers, the air mass stability upwind of the barrier, and upwind blocking. The orographic cloud component was determined by employing a simple parameterization which approximated the orographic forcing and attempted to account for blocking.

A serious difficulty encountered in a two-dimensional analysis of airflow past a ridge is the inability to describe the motion of air which fails to pass over the barrier due to: 1) downslope valley winds in lower levels (Reid, 1976), 2) stagnation due to valley inversions (Kao, 1965), 3) cold air pooling (Orgill, 1971), 4) light surface winds (Wong and Kao, 1970), 5) winds which encounter the barrier and turn parallel to it without ascending (Rhea, 1978), or 6) low level jets (Parish, 1982). If the lowest atmospheric layers are blocked from ascending the barrier, the upwind airflow will be displaced less than the topographical height of the barrier and the vertical velocities will be affected. Consequently, the condensate production rate would be modified. An example of this blocking phenomena affecting the airflow can be found in Rauber (1981).

The criteria for blocking chosen for this study was similar to that of Rhea (1978). A layer was termed blocked if the transbarrier wind component was less than  $2.0 \text{ m s}^{-1}$  or if  $dT/dP$  was less than  $0.4 \text{ K}/5.0 \text{ kPa}$ .

Table 2 illustrates the simple orographic lifting parameterization. The primary lift is defined as the ascent that air near the surface undergoes in order to be raised over the barrier, i.e., 10.0 kPa if no blocking is present. If blocking is present, the primary lift is reduced by the thickness of the blocked layer (see Fig. 4). The parameterization has the following features: 1) blocking can be accounted for and 2) streamline displacement decreases with height up to 40.0 kPa so that a decrease of lift with height is accounted for. The 40.0 kPa criteria was arbitrarily defined for application to the layers which could become cloudy after lifting over the bar-

TABLE 2. Orographic lifting parameterization.

Layer From the top of the blocked layer or from the surface (80 kPa) to ridge top (70 kPa) (kPa)†	Lift  Primary lift
70.0 to 60.0	1/2 · Primary lift
60.0 to 52.5	1/4 · Primary lift
52.5 to 45.0	1/8 · Primary lift
45.0 to 40.0	1/16 · Primary lift

† 1000 mb = 100 kPa.

rier. The moist air is important to this study and most of it lies below the "lid level". Note that the lifting parameterization simply describes to what level the air is lifted and does not describe the path the air takes as it flows up and over the mountain barrier. This lifting parameterization is reasonable under stable air-mass conditions as compared to airflow model results (Orgill, 1971; Mahrer and Pielke, 1975; Rhea, 1978). However, the parameterization is incapable of describing vertical velocity contributions from convection, synoptic forcing, differential advection, or mid-level descent. The orographic cloud components were determined by 1) lifting the upwind soundings with the simple lifting parameterization, and then 2) analyzing those lifted soundings for saturation with respect to water and ice.

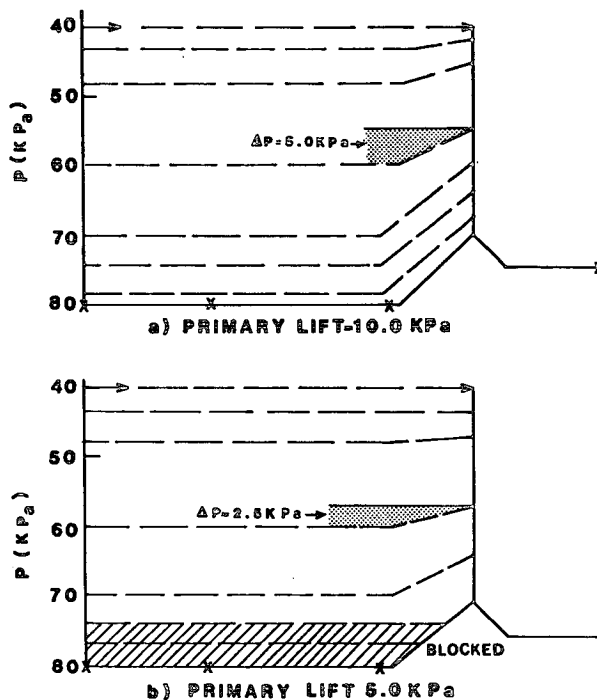


FIG. 4. X-Z cross section of the orographic parameterization: (a) no blocking and (b) blocked depth = 5.0 kPa.

Since the lifting model can only describe the first order effects of the orographic forcing, it is only a crude model at best. It is incapable of accounting for any deviation of the airflow caused by differential advection and stability changes, mid-level descent, pressure gradient forces, convective motions or synoptic scale vertical velocities. In order to test the sensitivity of this crude lifting model, an analysis using a modified lifting model was attempted using the soundings of Case Study 1. In the modified model, the primary lift was apportioned linearly between the surface and 30 kPa. This alternate lifting model effectively increased the lifting at all levels with a maximum deviation of 3.5 kPa at the 60 kPa level. In general, cloud tops were only slightly higher. However, in one case, the cloud tops deviated by as much as 7.5 kPa. These sensitivity tests show that the lifting model is less accurate under conditions when the dew-point depression increases very slowly with height. However, when there is a sharp drop off of moisture with height and stability effects (mid-level descent, convective motions, differential advection) are minimal, a greater confidence can be placed in this lifting approach.

The convective cloud components were determined by: 1) analyzing equivalent potential temperature ( $\theta_e$ ) as a function of height from the upwind, unlifted soundings and then, 2) analyzing the lifted soundings for saturation with respect to water. The layers in which  $d\theta_e/dZ < 0$  and became saturated with respect to water after lifting, were categorized "convectively unstable".

Differential advection effects are difficult to estimate and no doubt affect the stability profile and airflow structure. Representative soundings are provided with each case study to illustrate the stability changes that occurred during each storm.

Even though the lifting model results agree favorably with the case studies presented here, future investigations should approach orographic lifting with numerical models that can calculate the airflow structure with greater accuracy.

#### 4. Case studies

##### a. 1900 GMT 10 December to 0000 GMT 12 December 1979

The first case study analysis was performed on a well organized short wave system that passed over the study area on 10 and 11 December 1979. The upper air disturbance, most evident at 70 kPa, consisted of a strong short wave which moved through the study area at 0300 GMT on the 11th. Since this disturbance moved so quickly, it produced heavy precipitation for a relatively short time.

Figure 5 illustrates the 0300, 0600, and 0900 GMT soundings taken from Craig. This analysis of the soundings reveals the detailed temperature and moisture structure of the storm. Note the strong cooling in the lowest 20 kPa as the disturbance passed.

Figure 6a shows the time section of potential temperature and equivalent potential temperature as derived from the Craig rawinsonde. Note the development of a strong stable layer below the 60 kPa level after the front passed at 0300 GMT on the 11th.

Figure 6b shows the time section of the winds. Air flow in the lowest layers at Craig was strong enough so that at Craig, blocking was not present. After the front passed, the winds at the 70 kPa level veered to the northwest as the stable layer became established. Note the wind shear between 70 kPa and 50 kPa through the stable layer. Even though the flow was not blocked at Craig, the air closer to the barrier may indeed have been affected by a stagnation effect. However, no observations are available to support this suggestion. If stagnation and blocking are important factors in determining orographic lift, then observations at several distances upstream from the main barrier are necessary.

Figure 7a displays the time-height cross section of the synoptic component, the orographic component, and the blocking analysis. Rawinsondes were launched from Craig at 1900 and 2100 GMT 10 December, 0000, 0300, 0600, 0900, 1200, 1500 and 1800 GMT 11 December, and 0000 GMT 12 December 1979. Strong northwesterly winds at all levels provided a good low level lift and efficiently funneled the air into the western end of the Yampa Valley so that upwind blocking was not a dominant factor. Note that prior to 0000 GMT 11 December 1979, an orographic cloud formed over the barrier between 1.2 km and 5.0 km. At this time, the synoptic cloud component, layers saturated with respect to ice as deduced from uplifted, upwind soundings, had not yet formed.

The following visual observations confirmed the analysis results early in the storm period (all times GMT)

2130—A few layer clouds are forming over the ridge. Clear at Craig.

2300—Cirrus and stratus clouds invading the valley from the west at Craig. Small cumuli are forming over the ridge with the existing layer clouds.

0000—Altostratus clouds invading the valley from the west at Craig. A thick orographic cloud has formed over the ridge.

The ice saturated region of the orographic component above 6.0 km from 0000 to 0600 GMT on the 11th was simply due to advection of the synoptic component from the upwind position. At these altitudes there was no orographic lift as described by the simple lifting parameterization. The correlation between the onset of the analyzed synoptic cloud component and visual observations taken at Craig is good.

Figure 7b illustrates the time-height cross section of the orographic component, the convective com-

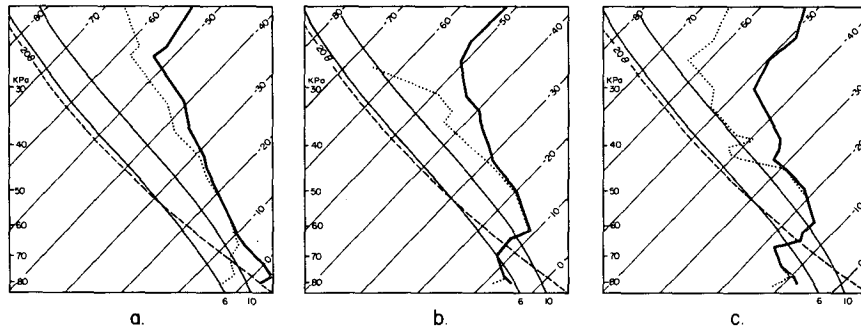


FIG. 5. Temperature (solid line) and dew point (dotted line) sounding for (a) 0300, (b) 0600 and (c) 0900 GMT 11 December 1979.

ponent, and the vertically pointing  $K_a$  band radar observations. Agreement between the radar observations and the orographic cloud analysis appears reasonable except that: 1) the radar failed to observe the water saturated cloud prior to 0300 on the 11th, 2) the radar

failed to detect the ice saturated region of the orographic cloud between 0300 and 0600 on the 11th. The first discrepancy may be due to the fact that the cloud existed only over the ridge and did not form far enough upwind for radar (situated at the base of the upwind mountain slope) to observe it. The second discrepancy may be due to the fact that the air was saturated with respect to ice but the ice crystals (if at all present) were too small or too few in number for detection by the radar.<sup>2</sup>

The convective component appears weak and embedded within the orographic component. A comparison of the convective instability, analyzed in Fig. 7b, and the  $K_u$  band radar reflectivity data presented in Fig. 8 shows reasonable agreement in time between the region of instability and the higher reflectivity values. However, the unstable layer was centered at 4.0 km while the higher reflectivities occurred closer to 2.0 km. It is hypothesized that ice crystals, falling from the zone of convective instability, fell into the dendritic crystal growth region,  $-14^\circ\text{C}$  to  $-17^\circ\text{C}$  (not shown here), and were responsible for the higher radar reflectivities at this time. (Further details concerning temperature cross sections and soundings are documented in Lee, 1980.)

Figure 7c depicts the precipitation record from three of the gages that were placed across the Park Range barrier. All of the precipitation was postfrontal and the highest precipitation rates developed quickly in concert with the mid-level convective cloud component and then decreased slowly in time. The fact that the snow started sooner at the highest elevation, easternmost sites before the trough passed suggests that this precipitation was probably not due to the synoptic precipitation component. Snow did not begin to fall at Craig until 0430 GMT February 11. If a synoptic component had been present at this time, the valley gages should have recorded some precipitation also.

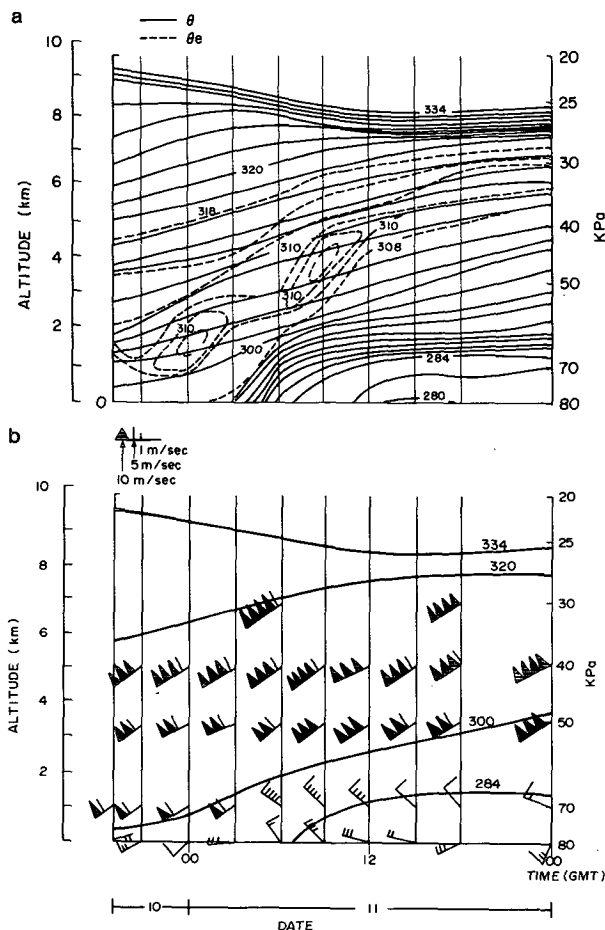


FIG. 6. Time-height cross section for case study 1 for (a) potential temperature (solid lines) and equivalent potential temperature (dashed lines), and (b) wind (barbs) and selected isotherms of potential temperature (solid lines).

<sup>2</sup> The  $K_a$  band radar had a peak power of 100 kW, a pulse rate of  $0.5 \mu\text{s}$ , a pulse repetition frequency of 1000 Hz, and a minimum detectable signal of  $104 \pm 3 \text{ dB}$ .

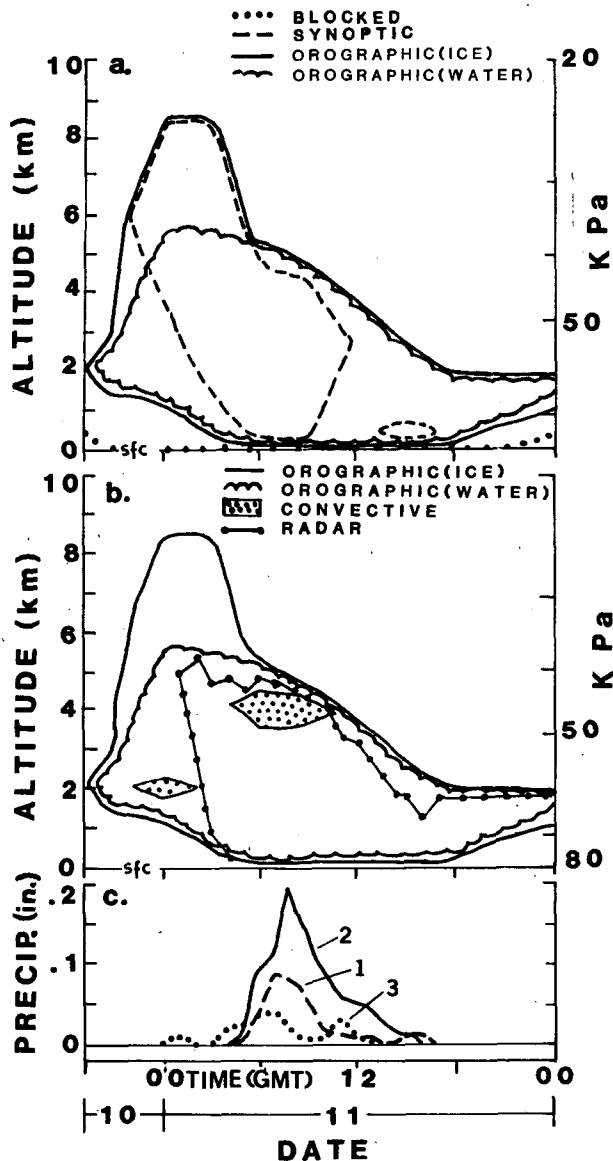


FIG. 7. Time-height cross-section for case study 1, from 1900 GMT 10 December to 0000 GMT 12 December 1979: (a) blocking analysis, synoptic, orographic ice and orographic water cloud components and (b)  $K_a$  radar cloud boundaries, convective, orographic ice, and orographic water cloud components; (c) Precipitation record (same time interval). See Fig. 3 for gage locations.

*b. 1200 GMT 22 February to 1800 GMT 24 February 1979*

The second case was performed on a long wave system. Fig. 9 shows three selected soundings that were taken at Craig. Note how the atmosphere dried out between 0600 and 2100 GMT on the 23rd and then moistened again by 0300 GMT on the 24th when the front passed through the study area.

Figure 10a shows the upwind time sections of potential temperature and equivalent potential temperature. The temperature gradients were much weaker than in the previous short wave case since this long wave moved much slower. The cooling in the lower levels between 0600 and 1200 GMT on the 23rd may be attributed to nocturnal cooling and cold air pooling. Radiative effects were not large this night due to a high overcast with light snow flurries. However, a valley inversion did form and was detected at Craig with the 1200 GMT sounding (see Fig. 11).

Figure 10b illustrates the time section of winds as derived from the Craig rawinsonde data. Notice that at times, below ridge top, the airflow did not have a flow toward the barrier. The blocking prior to frontal passage between 0600 GMT and 1200 GMT seems to have been produced by a local down valley drainage flow below a nocturnal inversion. This conclusion is supported by the rawinsonde data in that a valley inversion formed in conjunction with cooling of the temperature fields in time. These observations strengthen the argument for diurnal valley airflow and cold air pooling which contributes to blocking. This low level flow in turn can affect the orographic component of lift at the midlevels.

Frontal passage occurred near 0000 GMT 24 February. At this time, the synoptic airflow at ridge top level, 70 kPa, was strong out of the southwest. This produced a cross-valley flow and the air was not efficiently funneled into the western end of the Yampa Valley and then over the ridge. Consequently, the lower layers of air were stagnated and blocked from being lifted over the barrier.

Figure 12a displays the synoptic component, the orographic component, and the blocking analysis of the second case study. Rawinsondes were launched from Craig at 1200 and 1800 GMT 22 February, 0000, 0600, 1200, 1800 and 2100 GMT 23 February and 0000, 0300, 0600, 1200 and 1800 GMT 24 February 1979. Once again an orographic component formed over the barrier before the synoptic component provided ice saturated layers at the rawinsonde site. The following visual observations taken in the COSE study area on 22 February 1979 agree favorably in time with the analyzed orographic and synoptic cloud components:

- 1600 GMT—Skies are clear over the valley west of Hayden. Snow is falling on the ridge. The orographic cloud base is well below ridge top.

- 2030 GMT—The valley has just become overcast with stratus at Craig.

Between 1200 and 1800 GMT on the 23rd, slight ridging on the large scale wave occurred over the study area (Fig. 13) and barrier blocking restricted the airflow in the lower layers (Fig. 12a). Synoptic ridging suppressed the synoptic scale vertical velocities while the

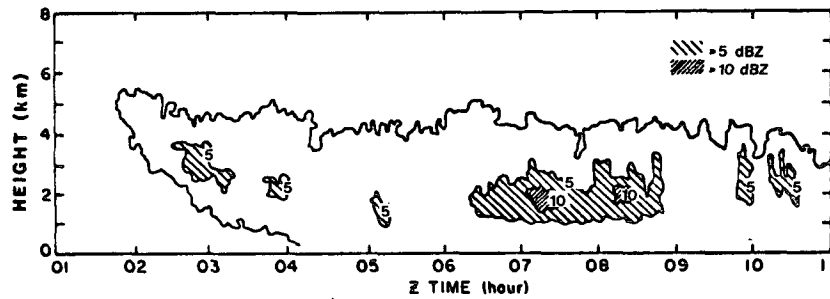


FIG. 8. Radar reflectivities for  $K_u$  band of case study 1 from 0100 to 1100 GMT 11 December 1979.

blocking restricted the low level orographic lift. Consequently, the orographic and synoptic components became shallower.

The synoptically produced ice saturated region near 3.8 km may have supplied ice crystals to the lower cloud layers over the barrier. This secondary source of ice crystals may have been important in reducing the seedability of this storm system.

Figure 12b illustrates the orographic component, the convective component, and the  $K_a$  band radar observations. At times the agreement between the radar cloud tops and the analyzed orographic cloud tops appears poor. However, agreement is reasonable at the times that the soundings were taken [0000, 0600, 2100 GMT 23 February and 0000, 0300 GMT 24 February 1979]. At 0600 and 1200 GMT on 24 February, the agreement between the  $K_a$  radar observations and the rawinsonde analysis is not good. This disparity may be due to: 1) the definition of cloud boundaries employed herein may be inadequate, 2) the lifting parameterization failed to simulate the environmental conditions, or 3) the cloud system may have been invigorated by some disturbance still unaccounted for. The zones of enhanced  $K_u$  band reflectivity, between 0400 and 1200 GMT 24 February in Fig. 14b supports the third explanation above.

The convective component appears stronger in this storm system than in the previous case study. The  $K_u$  band reflectivity data presented in Fig. 14 supports

this conclusion. The following visual observation, taken from a cloud physics research aircraft on 23 February 1979, supports the analysis in that some convective motions were present:

2333 GMT—The cloud tops look cumuliform. To the west, over the valley, stratiform decks are higher than the cumulus deck.

Figure 12c depicts the continuous precipitation record for this second case study. From 0000 to 0900 GMT on the 23rd the higher elevation precipitation gages recorded several “pulses” of precipitation. This observation roughly corresponds in time with the variable cloud top heights depicted by the  $K_a$  band observations in Fig. 12b and the zones of higher reflectivity embedded in a larger cloud mass ( $K_u$  band data) shown in Fig. 9a. One satellite photo, taken at 0000 GMT on the 23rd, revealed a small scale organization of several cloud lines (wavelength  $\sim 100$  km) embedded in a uniform cloud mass oriented northwest-southeast over the Park Range of Colorado. All of these observations suggest that the established cloud system may have been perturbed by a propagating mesoscale disturbance which was associated with the synoptic storm structure. Unfortunately, microbarograph observations were not available. The precipitation which fell between 0600 and 1200 GMT on 24 February (Fig. 12c), the  $K_u$  reflectivity data (Fig. 14b) and the small undulations in the  $K_a$  band cloud top

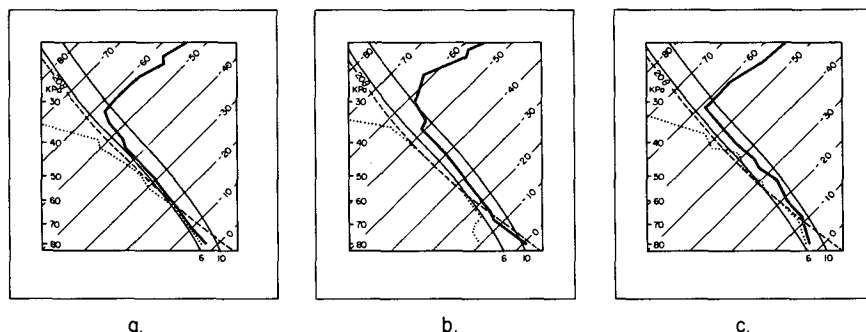


FIG. 9. As in Fig. 5 but for (a) 0600, (b) 2100 and (c) 0300 GMT 23 February 1979.



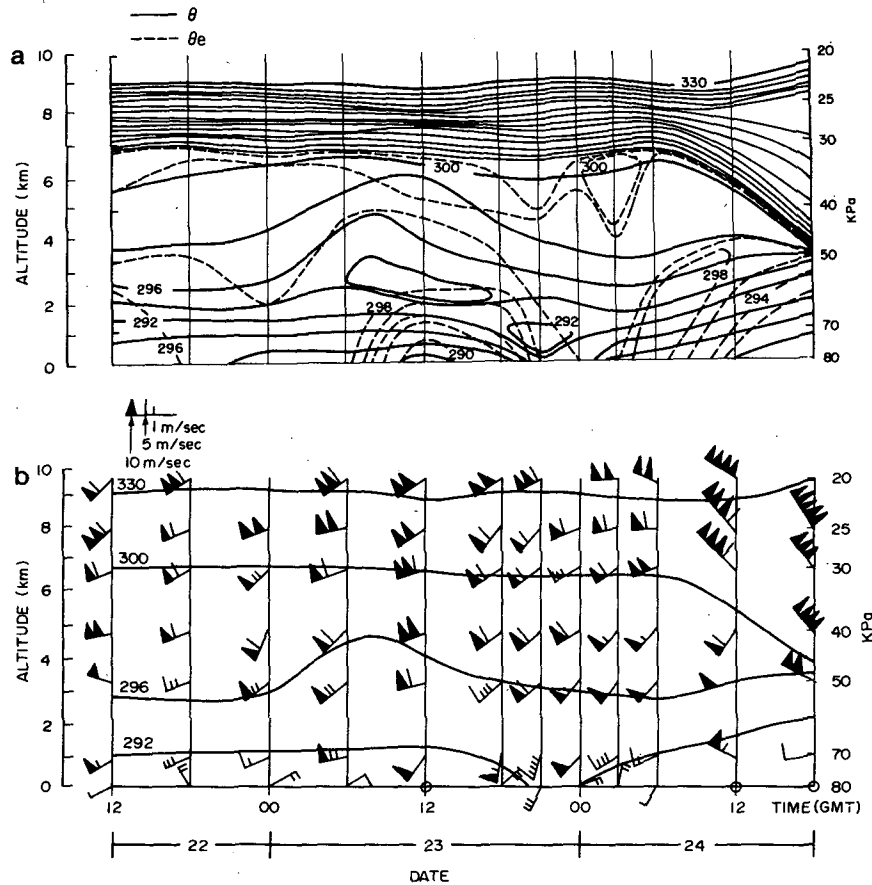


FIG. 10. As in Fig. 6 but for case study 2.

observations between 0500 and 1200 GMT (Fig. 12b) suggests that the existing cloud system may again have been affected by a propagating mesoscale disturbance.

## 5. Conclusions

Wintertime cloud systems over the Colorado Rockies consist of cloud components that, in turn, are generated by air which is forced vertically to condensation by different physical processes. Synoptic scale cloud components are determined by differential vorticity advection and air mass lifting by frontal systems. Orographic cloud components are determined by stable airflow that is forced vertically by the topography. Convective cloud components are determined by the release of convective instability as layers of air are lifted to saturation and differential advection by the synoptic disturbance. These vertical air motions combine constructively and destructively in time and space to produce the individual characteristics of each cloud system.

It is significant that the second case study radar, precipitation and satellite data indicated that the cloud system may have been modified by a mesoscale disturbance. This implies that at times, a fourth cloud

forming component (such as a traveling mesoscale gravity wave) is also important (Lindzen and Tung, 1976; Houze *et al.*, 1976). Further observations of how these traveling waves affect the pre-existing cloud systems are necessary. If mesoscale disturbances have a strong effect on orographic cloud systems, then microbarograph observations are important and should be included in future projects.

The time section analyses were sensitive to the lifting parameterization and the upwind profiles of temperature and moisture. This conclusion illustrates how important the lifting scheme is for accurate diagnoses or modeling of spatial cross sections of these cloud systems. Numerical models that calculate airflow structure should be employed in future studies.

Barrier blocking is an important phenomena which should be accounted for when modeling or parameterizing airflow over a ridge. Previous research (Kao, 1965; Wong and Kao, 1970; Fraser *et al.*, 1973; Rhea, 1978) has pointed out the importance of the blocking phenomena. These case studies have shown the effects that blocking has upon an orographic cloud system.

In the early stages of cloud system development, a pure orographic cloud formed over the ridge while upwind, over the valley, the skies remained clear. The

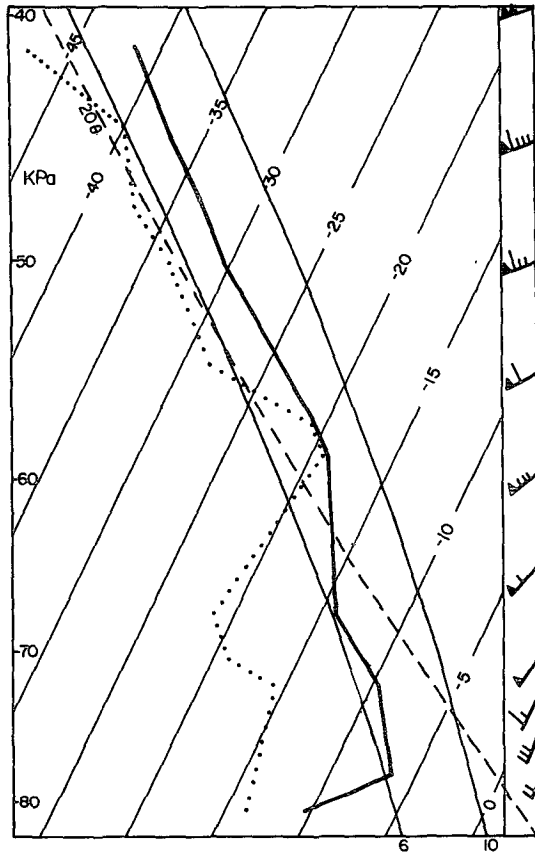


FIG. 11. As in Fig. 5 except for 1200 GMT 23 February 1979. Wind scale as in Fig. 6b or 10b.

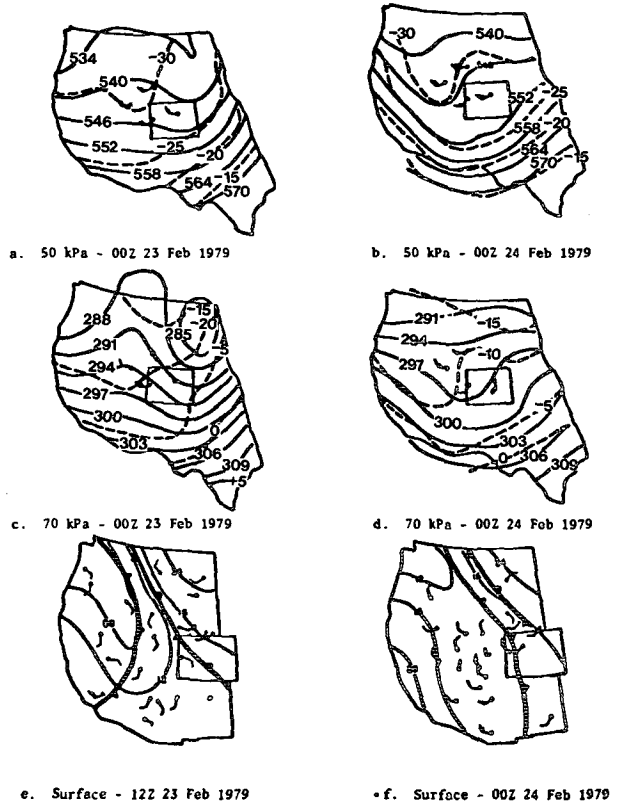


FIG. 13. Synoptic analysis for case study 2.

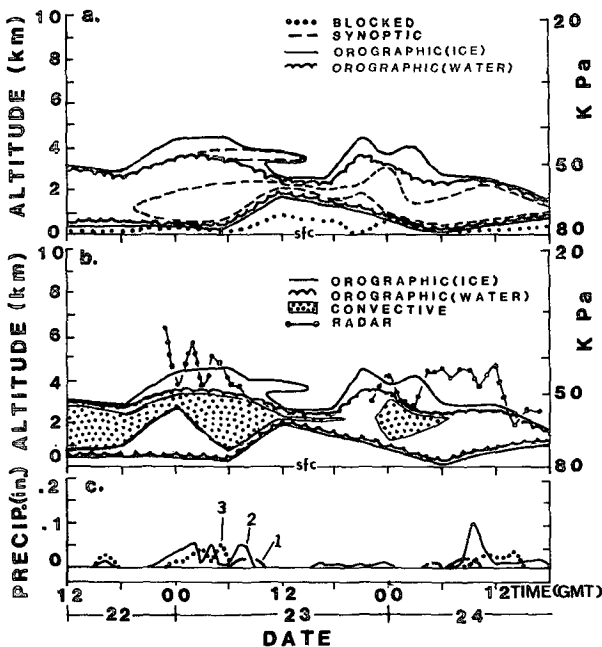


FIG. 12. As in Fig. 7 but for case study 2 from 1200 GMT 22 February to 1800 GMT 24 February.

correlation between rawinsonde analyzed synoptic cloud components and visual observations at Craig was good. This result suggests that it is reasonable to use ice saturation as a criteria for "cloud" from rawinsonde data during winter conditions. However, further comparison between rawinsonde analysis and aircraft observations are desirable.

In the second case study, the radar cloud tops appeared generally higher than the analyzed cloud tops. This suggests that the orographic cloud system had been affected by the atmospheric processes unaccounted for by the analysis: 1) convective elements changing the dynamics of the stable system, 2) synoptic scale vertical velocities interacting with the orographic vertical velocity field and 3) the gravity waves discussed previously. Smith (1970) and Grant and Elliott (1974) point out that convective elements that penetrate to higher and colder levels activate more ice nuclei and produce many more natural ice crystals than would have been produced under stable conditions.

Both case studies illustrated how convection may be superimposed upon the cloud system and that this instability can be caused by a combination of destabilization by synoptic scale advective processes, differential advection, and air mass lifting by the topography. These same points were made by Chappell (1970).

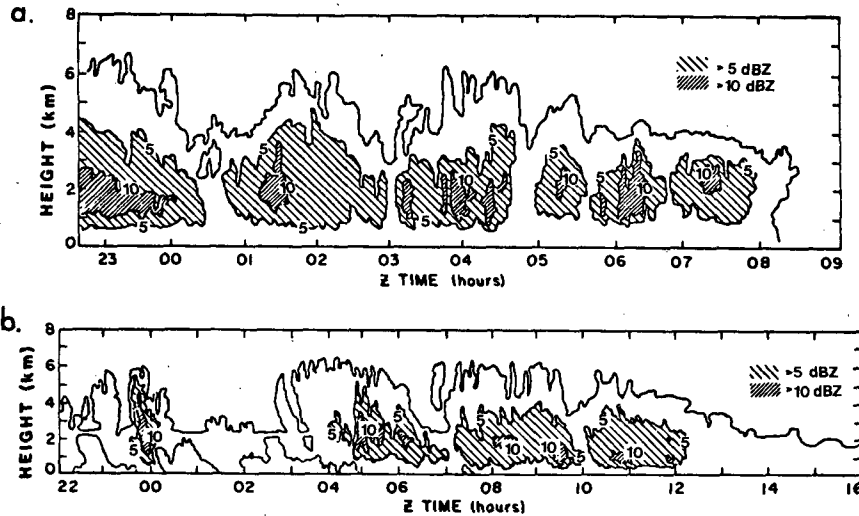


FIG. 14. As in Fig. 8 but for case study 2 (a) from 2230 GMT 22 February to 0900 GMT 23 February 1979 and (b) from 2300 GMT 23 February to 1600 GMT 24 February 1979.

Formation and interaction between the four cloud components defines the structure and characteristics of the complete orographic cloud system. The physical processes associated with each cloud component controls the interaction between the atmosphere and the mountainous terrain which produces each characteristic orographic cloud system and the accompanying precipitation.

**Acknowledgments.** This research was completed as partial fulfillment of a Master of Science degree at Colorado State University under the supervision of Professor Lewis O. Grant. Further details can be found in CSU Atmospheric Science Paper 331. The  $K_a$  band radar was provided to COSE II by the National Oceanic and Atmospheric Administration. I would also like to thank Mr. Joseph Greeson of Colorado State University for his reduction of the  $K_a$  band radar data. This work was supported by the National Science Foundation Grants ATM 7819261 and ATM 8109590. The author gratefully acknowledges the time provided by the Air Force Geophysics Laboratory to prepare this paper for publication.

#### REFERENCES

- Chappell, C. F., 1970: Modification of cold orographic clouds. Ph.D. dissertation, Dept. Atmos. Sci., Colorado State University, 196 pp.
- Elliott, R. D., 1966: Effects of seeding on the energy of systems. *J. Appl. Meteor.*, **5**, 663–668.
- , and R. W. Schaffer, 1962: The development of quantitative relationships between orographic precipitation and air mass parameters for use in forecasting and cloud seeding evaluation. *J. Appl. Meteor.*, **1**, 218–228.
- , and E. L. Hovind, 1964: On convection bands within Pacific coast storms and their relation to storm structure. *J. Appl. Meteor.*, **3**, 143–154.
- Fraser, A. B., R. C. Easter and P. V. Hobbs, 1973: A theoretical study of the flow of air and the fallout of solid precipitation over mountainous terrain. Part I: Airflow model. *J. Atmos. Sci.*, **30**, 801–812.
- Grant, L. O., and R. D. Elliott, 1974: The cloud seeding temperature window. *J. Appl. Meteor.*, **3**, 355–363.
- Houze, R. A., P. V. Hobbs, K. R. Biswas and W. M. Davis, 1976: Mesoscale rainbands in extratropical cyclones. *Mon. Wea. Rev.*, **104**, 868–878.
- Kao, T. W., 1965: The phenomenon of blocking in stratified flows. *J. Geophys. Res.*, **70**, 815–822.
- Lee, R. R., 1980: Wintertime cloud systems over the Colorado Rockies; Three Case Studies. Master's thesis, Atmos. Sci. Pap. 331, Dept. Atmos. Sci., Colorado State University, 115 pp.
- Lindzen, R. S., and K. K. Tung, 1976: Banded convective activity and ducted gravity waves. *Mon. Wea. Rev.*, **104**, 1602–1617.
- Mahrer, Y., and R. A. Pielke, 1975: A numerical study of the airflow over mountains using the two-dimensional version of the University of Virginia mesoscale model. *J. Atmos. Sci.*, **32**, 2144–2155.
- Marwitz, J. D., 1974: An airflow case study over the San Juan Mountains of Colorado. *J. Appl. Meteor.*, **13**, 450–458.
- Orgill, M. M., 1971: Laboratory simulation and field estimates of atmospheric transport-dispersion over mountain terrain. Ph.D. dissertation, Dept. Civ. Eng., Colorado State University, 298 pp.
- Parish, T. R., 1982: Barrier winds along the Sierra Nevada Mountains. *J. Appl. Meteor.*, **21**, 35–40.
- Rauber, R. M., 1981: Microphysical processes in two stably stratified orographic cloud systems. Master's thesis, Atmos. Sci. Pap. 337, Dept. Atmos. Sci., Colorado State University, 154 pp.
- Reid, J., 1976: Dispersion in a mountain environment. Ph.D. dissertation, Atmos. Sci. Pap. 253, Colorado State University, 150 pp.
- Rhea, J. O., 1978: Orographic precipitation model for hydrometeorological use. Ph.D. dissertation, Atmos. Sci. Pap. 287, Colorado State University, 198 pp.
- Saucier, W. J., 1955: *Principles of Meteorological Analysis*. University of Chicago Press, 438 pp.
- Smith, E. J., 1970: Effects of cloud top temperatures on the results of cloud seeding with silver iodide in Australia. *J. Appl. Meteor.*, **9**, 800–804.
- Wong, K. K., and T. W. Kao, 1970: Stratified flow over extended obstacles and its application to topographical effects of vertical wind shear. *J. Atmos. Sci.*, **27**, 884–889.